Candidate screening of host cell membrane proteins involved in SARS-CoV-2 entry

**Norihiro Kotani[1*] and Takanari Nakano[1]**

From the [1]Department of Biochemistry, Saitama Medical University, 38 Morohongo, Moroyama-machi, Iruma-gun, Saitama 350-0495, Japan

*To whom correspondence should be addressed: Norihiro Kotani: Department of Biochemistry, Saitama Medical University, 38 Morohongo, Moroyama-machi, Iruma-gun, Saitama 350-0495, Japan; kotani@saitama-med.ac.jp; Tel: +81-49-276-1155; Fax: +81-49-276-1155

**Running title**: Membrane protein candidates involved in SARS-CoV-2 entry

**Keywords:** SARS-CoV-2, Membrane protein, Virus entry, Lipid raft, Proteomics, Protein-protein interaction.

## ABSTRACT

COVID-19 represents a real threat to the global population, and understanding the biological features of the causative virus (SARS-CoV-2) is imperative to aid in mitigating this threat. Analyses of proteins such as primary receptors and co-receptors (co-factors) that are involved in SARS-CoV-2 entry into host cells will provide important clues to help control the virus. Here, we identified host cell membrane protein candidates that were present in proximity to the attachment sites of SARS-CoV-2 spike proteins through the use of proximity labeling and proteomics analysis. The identified proteins represent candidate key factors that may be required for viral entry. Our results indicated that a number of membrane proteins, including DPP4, Cadherin-17, and CD133, were identified to co-localize with cell membrane-bound SARS-CoV-2 spike proteins in Caco-2 cells that were used to expand the SARS-CoV-2 virion. We anticipate that the information regarding these protein candidates will be utilized for the future development of vaccines and antiviral agents against SARS-CoV-2.

## INTRODUCTION

COVID-19, caused by the SARS-CoV-2 virus, was first reported in Wuhan, China, and now represents a threat to numerous individuals world-wide. SARS-CoV-2 is a member of *Coronaviridae*, and many of these coronaviruses have long been known to cause severe respiratory failure (1). It can therefore be inferred that cells within the respiratory organs are the growth sites for SARS-CoV-2 virions, and the analyses of virus receptors within these host cells have been performed. In addition to its ability to infect respiratory organs, SARS-CoV-2 can also infect vascular endothelium and the intestinal tract (2, 3), suggesting that these viral receptors are diverse. In SARS-CoV-1 (4, 5) and MERS-CoV (6), certain protease family proteins within host cells have been identified to act as primary receptors or co-receptor (co-factors) for

these viruses, and in particular ACE2 has been studied as a dominant candidate (7). Similarly, SARS-CoV-2 has been reported to target ACE2 and other cell surface proteins (8).

Other membrane proteins involved in virus entry should also be noted. The chemokine receptors CCR5 and CXCR4 have been reported as co-receptors involved in human immunodeficiency virus infection (9–11), and HLA class II receptors function as co-receptors in Epstein-Barr virus infection (12). The fields of vaccine and antiviral development are of interest in regard to viral co-receptors (co-factors) in addition to primary receptors (13). Therefore, host cell membrane proteins involved in SARS-CoV-2 attachment and entry should be broadly considered as the important key factors and therapy targets for SARS-CoV-2 infection. In the case of SARS-CoV-2, various host cell membrane proteins other than ACE2 have also been reported as factors that mediate viral entry (14, 15); however, the detailed mechanisms underlying their functions remain unknown. It is speculated that these factors are membrane proteins located in proximity to the viral attachment point (binding site of SARS-CoV-2 spike protein) in the host cell membrane.

The proximity labeling method (16–19) has recently been used as a method to analyze physiological protein interactions. We developed a simple physiological method termed the Enzyme-Mediated Activation of Radical Source (EMARS) method (20) that uses horseradish peroxidase (HRP)-induced radicals derived from arylazide or tyramide compounds (21). The EMARS radicals attack and form covalent bonds with the proteins in the proximity to the HRP (*e.g.* radicals from arylazide; approximately 200–300 nm (20), from tyramide; approx. 20 nm (22)), as the generated radicals immediately react with surrounding water molecules and disappear close to HRP. The labeled proteins can subsequently be analyzed using an antibody array and/or a typical proteome strategy (23). The EMARS method has been applied for various studies of molecular complexes on the cell membrane (24–31).

Proximity labeling typically analyzes intracellular molecular interactions to allow for observations of the proximity between free proteins. In contrast, EMARS is a tool for analyzing proximity molecules on the cell surface proteins, and using this method, it is highly possible that the key factor proteins located in proximity to the viral protein bound to the cell membrane at the initial stage of virus infection can be labeled. We therefore speculated that this method would provide a useful tool for identifying candidate molecules as a key factor of SARS-CoV-2 infection.

Here, we identified protein candidates that existed in close proximity to virus spike proteins bound to host cells in the early stage of SARS-CoV-2 infection by using the EMARS method and proteomics technology. The EMARS reaction was performed using the HRP-conjugated recombinant SARS-CoV-2 spike protein (S1-RBD) in A549 lung cancer cells and Caco2 cells. Caco2 cells are a commonly used cultured cell type that allow for efficient replication of SARS-CoV-2 virions. The labeled proteins identified as candidate membrane proteins were analyzed using proteomics technology.

## RESULTS

### Preparation of a SARS-CoV-2 spike protein probe for use in the EMARS reaction

To perform an EMARS reaction, an EMARS probe that possesses HRP that is conjugated to a given molecule that recognizes a target molecule is required (20). The HRP-conjugated SARS-CoV-2 spike protein corresponds to an EMARS probe in this study (Fig. 1A). The spike protein used in this study was a receptor-binding domain (RBD) that is present in the S1 protein of SARS-CoV-2 that possesses a mouse immunoglobulin Fc region (mFc) at the C-terminus (total 457 a. a.). We used the mFc sequence to conjugate HRP. We initially examined if the spike protein binds to host cells using Caco-2 and A549 cells. Caco-2 cells were treated with Alexa Fluor 488 fluorescent dye-conjugated monovalent spike proteins created using a commercial labeling kit, and labeling was then observed using a fluorescent microscope. We simultaneously prepared the sample that was created through incubation with intact spike protein-mFc followed by incubation with anti-mouse IgG-Alexa Fluor 488. Both samples exhibited binding of spike protein-mFc to the cells; however, the latter two-step staining procedure was found to be more effective (Fig. 1B). When each cell was fixed with 4% paraformaldehyde and then stained, the binding of spike proteins was considerably weakened (data not shown). Based on these results, a method for EMARS in this study was adopted in which the SARS-CoV-2 spike protein was directly applied to living cells that were then treated with HRP-conjugated anti-mouse IgG. Similar results were obtained using A549 cells; however, the binding of the SARS-CoV-2 spike protein was weaker than that observed using Caco-2 cells (Fig. 1B).

**EMARS and proteomic analysis revealed a number of candidate proteins**

As ACE2 is listed as the primary receptor for SARS-CoV-2, we examined the expression of ACE2 in Caco-2 and A549 cells. From western blot analyses, a clear band was observed at a molecular weight of approximately 100,000 Da in Caco-2 cells; however, this signal was faint in A549 cells (Fig. 2A). The cells also exhibited positive staining for ACE2 antibody, demonstrating that ACE2 could be observed in both cells; however Caco-2 cells appeared to exhibit higher expression (Fig. 2B). Additionally, Caco-2 cells exhibited strong staining of portions of the cell membrane, while A549 cells possessed a homogeneous staining pattern (Fig. 2B).

The EMARS reaction was performed in these cells using the EMARS probe described above. Following the EMARS reaction, the labeled molecules were subjected to SDS-PAGE. The gels used for electrophoresis can be analyzed directly using a fluorescence image analyzer when the labeled molecules are present in large amounts; however, the bands for the EMARS sample using the SARS-CoV-2 spike protein could not be clearly detected (Data not shown). The labeled molecules were therefore observed by western blot analysis using the anti-fluorescein antibody. The EMARS reaction was first performed in Caco-2 cells using HRP-conjugated cholera toxin subunit B as a positive control, as this conjugate is known to bind to a lipid raft structure on the cell membrane and can subsequently label numerous cell surface proteins (Fig. 2C). Using the SARS-CoV-2 spike protein, we performed the EMARS reaction in conjunction with some negative control experiments. Although weak bands were observed in the negative control (treated

with anti-mouse IgG-HRP antibody only; hereinafter referred to as spike [-] sample), the combination of both SARS-CoV-2 spike protein and anti-mouse IgG-HRP antibody (hereinafter referred to as spike [+] sample) yielded significant bands (Fig. 2C). As the signal was weaker compared to that obtained using the cholera toxin probe, it was possible that certain specific cell membrane proteins were labeled in a limited manner in the samples using the SARS-CoV-2 spike protein probe. For A549 cells, a number of labeled proteins were detected in the spike [+] sample; however, the band pattern was different compared to that obtained from Caco-2 cells (Fig. 2D).

These labeled proteins were subjected to proteomic analysis. There was a possibility that identification could not be sufficiently achieved using mass spectrometry, as the amount of labeled molecules was likely smaller than that obtained using the CTxB-HRP probe. Multiple independent experiments were therefore performed (twice for Caco-2 cells and three times for A549 cell), and the results were then combined and used for the analysis.

Spike [+] samples and spike [-] samples (as a negative control) were both prepared from each cell. For shotgun analysis using mass spectrometry, the labeled molecules were purified by immunoprecipitation with an anti-fluorescein antibody. A total of 181 proteins were detected in the spike [+] samples from Caco-2 cells, and 59 proteins were detected from the spike [-] samples (raw data; Supporting tables 1 and 2). A total of 184 proteins were detected in the spike [+] samples from A549 cells, and 186 proteins were detected from the spike [-] samples (raw data; Supporting tables 3 and 4). The molecules detected in the spike [-] sample may be proteins that were non-specifically adsorbed during the purification process. In particular, for unknown reasons, spike [-] sample from A549 cells contained many suspected non-specific binding proteins. Of the proteins in the spike [+] sample list, membrane proteins that were not present in the spike [-] sample list for each cell were preferentially specified as the most likely candidates in this study. In Caco-2 cells, 15 types of membrane proteins and partially cell surface proteins such as Cadherin 17 were listed as candidates (Table 1), and in A549 cells, 10 types of membrane proteins such as CD44 were listed.

**The identified membrane proteins co-localized with the SARS-CoV-2 spike protein**

We next examined if the identified membrane proteins co-localized with the SARS-CoV-2 spike protein bound to the Caco-2 cell membrane. Caco-2 cells were treated with SARS-CoV-2 spike proteins, and this was followed by staining with antibodies recognizing the above candidates. Representative images of ACE2, CD133, Cadherin 17, and DPP4 were summarized in Fig. 3. It was found that all of these proteins (red signals) were at least expressed in Caco2 cells and co-localized with the SARS-CoV-2 spike protein (green signals). Interestingly, it was observed that the co-localized area was limited at specific membrane sites, despite the observation that these proteins were expressed abundantly.

## DISCUSSION

To date, the possibility for the host cell proteins involved in SARS-CoV-2 replication to be used as

therapy targets has been reported according to proteomics-based analysis (32). However, as viral infection first occurs through the host cell membrane, it is also considered to be important to focus on membrane proteins such as the primary viral receptor. In particular, previous virus studies have suggested that lipid rafts, which are assembly structures consisting of several membrane proteins, are important for viral entry (33). Previous studies have demonstrated that the EMARS reaction used in this study is effective for identifying proximity proteins, including this lipid raft structure (34). It was therefore speculated that EMARS is suitable for investigating crucial membrane proteins located in the proximity region of the cell membrane-bound SARS-CoV-2 spike protein involved in virus entry.

It has been reported that SARS-CoV-2 easily expands in Caco-2 cells compared to expansion in A549 cells (8, 35). One of the reasons for these differences has been speculated to involve the differences in ACE2 expression levels observed in these cells. In the current study, ACE2 expression was clearly observed in CaCo-2 cells compared to observations in A549 cells (Fig. 2B), thus supporting the binding capacity of the SARS-CoV-2 spike protein in this study. In contrast, it has been also reported that the expression level of ACE2 in A549 cells is relatively high (36) and that virus attachment could occur even if the replication ability was low (35). Regardless, as the binding of the spike protein to A549 cells was observed in this study, it was concluded that the experiment could be performed in both Caco-2 and A549 cells.

For preparation of the EMARS probe, the binding capacity of the SARS-CoV-2 spike protein to the cell membrane was assayed. We expected to observe clear spike protein staining in Caco-2 cells due to the high ACE2 expression in this cell line. However, only a portion of the cell population was able to bind to the SARS-CoV-2 spike protein, and the other cells did not exhibit clear binding (Fig. 1B). Previous studies examining SARS-CoV-2 infection have suggested that even in homogeneous cell lines, the specimens were divided into infected and non-infected cells (2, 35). Even in HeLa cells that overexpress ACE2, not all cells were observed to be infected (37). This may reflect the events observed in this study, indicating that the cytological images of spike protein used in this study were similar to those of SARS-CoV-2 infection reported by other studies. The distinction of the binding among cultured cells is presumed to be due to the condition of each cell population (*e.g.* cell cycle, expression levels of co-receptor [co-factors] membrane proteins); however, the actual cause remains unknown.

The staining experiments implied that the amount of membrane proteins labeled by the EMARS reaction may be small. The labeling of molecules by EMARS was confirmed in both Caco-2 cells and A549 cells (Fig. 2C and 2D); however, the amount of labeled molecules was smaller than expected and could only be detected at the Western blot level. Considering the loss of the labeled protein in the purification process and the sensitivity of shotgun analysis by mass spectrometry, it was necessary to combine multiple samples obtained through multiple independent experiments despite the non-specific adsorption that occurs during the purification process. In A549 cells, a number of proteins that were expected to be non-specific adsorbed proteins were

detected in the negative control sample and were not subjected to the EMARS reaction (spike [-]). We therefore decided to select the candidate membrane proteins using a subtraction method that incorporated the membrane proteins present in the samples subjected to the EMARS reaction (spike [+]) in both cells (Table 1). Although there was a difference in the candidate proteins between Caco-2 cells and A549 cells, it was speculated that the membrane proteins that act as co-factors for SARS-CoV-2 entry were dependent upon cell origin. As SARS-CoV-2 is known to infect multiple cell types (2, 3, 35), these differences appear to be events that must to be considered in SARS-CoV-2 studies. In contrast, a number of identical proteins between Caco-2 and A549 cells, including the transferrin receptor protein and other (Table 1), were detected. These are ubiquitous proteins; however, they may still play an important role by acting as a common target against SARS-CoV-2 infection. However, it should also be considered that ubiquitous and highly expressed cell membrane proteins are more likely to be detected in proteomics. Another factor is that ACE2 could not be detected as a candidate protein in this study. This raises the issue of labeling efficiency for ACE2 by EMARS or of fluorescein covalent binding to ACE2. The latter is a possible issue to the observation that the binding of certain fluorophores can interfere with proteomic analyses.

Cadherin 17, which exhibited the highest score in Caco-2 cells, is a member of the cadherin superfamily that mediates $Ca^{2+}$-dependent cell–cell adhesion without the connection to a cytoskeleton molecule. The physiological functions of Cadherin 17 include the ability of this protein to act as a regulator of B cell development according to a knockout mouse study (38). It has been also reported that Cadherin 17 can influence the progression of certain cancers (39, 40); however there have been almost no reports on the relationship between Cadherin 17 and viral infection. Neither Prominin-1 (CD133) (41) nor Glypican-3 (42) has at least been reported to be related to viral infection, including SARS-CoV-2 infection. Transferrin has been reported as a co-receptor for the hepatitis C virus (43), but its relationship to SARS-CoV-2 infection has not been reported. In contrast, it has been reported that DPP4 (44) and Heterogeneous nuclear ribonucleoprotein (45) affect SARS-CoV-1 and/or SARS-CoV-2 infections (46, 47). In A549 cells, CD44 (48), Contactin1 (49), Cadherin-1 (50), and Reticulon-4 receptor-like 2 (51) have not yet been reported to exhibit any relationship to SARS-CoV-2 infection. In contrast, it has been reported that integrin families act as co-receptors for other viruses (52, 53), and it has subsequently been noted that these proteins exhibit a relationship to SARS-CoV-2 infection (54, 55). Interestingly, while carcinoembryonic antigen-related cell adhesion molecule (CEACAM) (56, 57) has been speculated to act as a primary receptor of mouse coronavirus (58), a recent network perturbation analysis suggested a very specific influence of this molecule in SARS-CoV-2 infection (59). Our findings obtained in this study, including those regarding CEACAM, and the observed concordance of our study results with those of previous studies indicate that potent candidate proteins can be obtained through the use of our method.

The results of the confocal microscopy experiment (Fig. 3) revealed

that the candidate proteins co-localized with the spike protein however, the co-localization was not identical. It is possible that this is attributable to the contribution of multiple factors (*e.g.* influence of the plasma membrane environment) other than the identified candidate proteins. It is unclear if the strength of spike protein binding is directly associated with SARS-CoV-2 infection efficiency.

In conclusion, the candidate target proteins identified in this study were partially consistent with the results obtained by previous SARS-CoV-2 studies. Our method is therefore considered to be effective as a tool for identifying the host cell membrane proteins involved in virus infection. Additionally, it is necessary to examine in detail if the candidate proteins newly identified in this study are the factors that control SARS-CoV-2 infection. We hope that the results of this study will help to elucidate the viral entry mechanism of SARS-CoV-2 and to develop novel therapeutic agents in future.

## Experimental Procedures

Portions of the "*Experimental procedure*" are contained in the Supporting Information.

### *EMARS reaction*

The EMARS reaction and the detection of EMARS products were performed as described previously (20). Briefly, Caco-2 and A549 cells were cultured in 10 cm plastic culture dishes (TPP) until approximately 80-90 % confluent, and they were then washed once with PBS at room temperature and subsequently treated with HRP-conjugated Cholera Toxin B Subunit B (CTxB-HRP; LIST Biological Lab) or SARS-CoV-2 spike protein (0.5 μg/ml 2% BSA-PBS) at room temperature for 30 min. After washing with PBS three times the cells were treated with HRP-conjugated anti-mouse IgG (W402B; Promega; 0.25 μg/ml 2% BSA-PBS) at room temperature for 30 min. After gently washing the cells five times with PBS, the treated cells were then incubated with 0.05 mM fluorescein-conjugated tyramide (FT) (21) with 0.0075% $H_2O_2$ in PBS at room temperature for 10 min in dark. The cell suspension was homogenized through a 22 G syringe needle to rupture the plasma membranes, and the samples were centrifuged at 20,000 g for 15 min to precipitate the plasma membrane fractions. After solubilization using NP-40 lysis buffer (20 mM Tris-HCl (pH 7.4), 150 mM NaCl, 5 mM EDTA, 1% NP-40, 1% glycerol), the samples were subjected to SDS-PAGE as described above.

### *Proteomic analysis of EMARS products using mass spectrometry analysis*

Proteomic analysis was performed using nano-liquid chromatography-electrospray ionization mass spectrometry (nano LC-ESI-MS/MS). The eluted samples described above were treated with a final 10 mM concentration of DTT (Wako Chemical) at 50°C for 30 min, and they were then treated with 50 mM iodoacetamide (Wako Chemical) in 50 mM ammonium carbonate buffer at 37°C for 1 h. To remove SDS, SDS-eliminant (ATTO) was directly added to the samples, and the samples were incubated at 4°C for 1 h. After centrifugation, the supernatant was transferred to a new tube and then digested with 2 μg of trypsin (Trypsin Gold MS grade; Promega) at 37°C overnight. For peptide purification, the digested sample was applied to a C18-StageTip (GL Science) according to

the manufacturer's instructions. The sample was solubilized in 10 μL of 2% acetonitrile (ACN)/0.1% formic acid/H2O solution. The prepared samples were injected into an Ultimate 3000 RSLCnano (Thermo Fisher Scientific). Mass analysis was performed using a LTQ Orbitrap XL mass spectrometer equipped with a nano-ESI source (Thermo Fisher Scientific). A NIKKYO nano HPLC capillary column (3μm C18, 75 μm I.D.×120 mm; Nikkyo Technos) was used, and this was preceded by a C18 PepMap100 column (300 μm I.D × 5mm; Thermo Fisher Scientific). The peptides were eluted from the column using a 4% to 35% acetonitrile gradient over 97 min. The eluted peptides were directly electro-sprayed into the spectrometer, and were subjected to precursor scan and data-dependent MS/MS scan.

The raw data were analyzed using Proteome Discoverer ver. 2.4 software (Thermo Fisher Scientific) with the following parameters: Cys alkylation: iodoacetamide, Digestion: Trypsin, Species: Homo sapiens or Mus musculus, FDR (False discovery rate): strict 1%, relaxed 5%, respectively. The classification of the identified proteins as membrane protein was accomplished according to the UniProt database.

**Data availability**: The data supporting our findings are available in this article and supporting information.

**Acknowledgements**: We thank Ms. Amimoto of the Natural Science Center for Basic Research and Development (N-BARD), Hiroshima University, for MS technical assistance and we thank the Saitama Medical University Biomedical Research Center for providing general technical assistance.

**Conflict of Interest**: The authors declare that they have no conflicts of interest regarding the contents of this article.

**Funding**: This work was supported by Grants-in-aid for Scientific Research in Japan (No. JP18K06663 to N. K.).

**Author Contributions**: Conceptualization, N.K.; Methodology, N.K..; Investigation, N.K. and T.N.; Resources, N.K. and T.N. Data Curation, N.K.; Writing-Original Draft, N.K. and T.N.; Writing - Review & Editing, N.K., T.N.; Supervision, N.K.; Funding Acquisition, N.K.

## REFERENCES

1. Zhu, N., Zhang, D., Wang, W., Li, X., Yang, B., Song, J., Zhao, X., Huang, B., Shi, W., Lu, R., Niu, P., Zhan, F., Ma, X., Wang, D., Xu, W., Wu, G., Gao, G. F., and Tan, W. (2020) A novel coronavirus from patients with pneumonia in China, 2019. *N. Engl. J. Med.* **382**, 727–733
2. Lamers, M. M., Beumer, J., van der Vaart, J., Knoops, K., Puschhof, J., Breugem, T. I., Ravelli, R. B. G., Paul van Schayck, J., Mykytyn, A. Z., Duimel, H. Q., van Donselaar, E., Riesebosch, S., Kuijpers, H. J. H., Schipper, D., van de Wetering, W. J., de Graaf, M., Koopmans, M., Cuppen, E., Peters, P. J., Haagmans, B. L., and Clevers, H. (2020) SARS-CoV-2 productively infects human gut enterocytes. *Science*. **369**, 50–54
3. Varga, Z., Flammer, A. J., Steiger, P., Haberecker, M., Andermatt, R., Zinkernagel, A. S., Mehra, M. R., Schuepbach, R. A., Ruschitzka, F., and Moch, H. (2020) Endothelial cell infection and endotheliitis in COVID-19. *Lancet*. **395**, 1417–1418
4. Ksiazek, T. G., Erdman, D., Goldsmith, C. S., Zaki, S. R., Peret, T., Emery, S., Tong, S., Urbani, C., Comer, J. A., Lim, W., Rollin, P. E., Dowell, S. F., Ling, A. E., Humphrey, C. D., Shieh, W. J., Guarner, J., Paddock, C. D., Roca, P., Fields, B., DeRisi, J., Yang, J. Y., Cox, N., Hughes, J. M., LeDuc, J. W., Bellini, W. J., and Anderson, L. J. (2003) A novel coronavirus associated with severe acute respiratory syndrome. *N. Engl. J. Med.* **348**, 1953–1966
5. Drosten, C., Günther, S., Preiser, W., Van der Werf, S., Brodt, H. R., Becker, S., Rabenau, H., Panning, M., Kolesnikova, L., Fouchier, R. A. M., Berger, A., Burguière, A. M., Cinatl, J., Eickmann, M., Escriou, N., Grywna, K., Kramme, S., Manuguerra, J. C., Müller, S., Rickerts, V., Stürmer, M., Vieth, S., Klenk, H. D., Osterhaus, A. D. M. E., Schmitz, H., and Doerr, H. W. (2003) Identification of a novel coronavirus in patients with severe acute respiratory syndrome. *N. Engl. J. Med.* **348**, 1967–1976
6. Zaki, A. M., van Boheemen, S., Bestebroer, T. M., Osterhaus, A. D. M. E., and Fouchier, R. A. M. (2012) Isolation of a Novel Coronavirus from a Man with Pneumonia in Saudi Arabia. *N. Engl. J.*

*Med.* **367**, 1814–1820

7. Li, W., Moore, M. J., Vasllieva, N., Sui, J., Wong, S. K., Berne, M. A., Somasundaran, M., Sullivan, J. L., Luzuriaga, K., Greeneugh, T. C., Choe, H., and Farzan, M. (2003) Angiotensin-converting enzyme 2 is a functional receptor for the SARS coronavirus. *Nature*. **426**, 450–454
8. Hoffmann, M., Kleine-Weber, H., Schroeder, S., Krüger, N., Herrler, T., Erichsen, S., Schiergens, T. S., Herrler, G., Wu, N. H., Nitsche, A., Müller, M. A., Drosten, C., and Pöhlmann, S. (2020) SARS-CoV-2 Cell Entry Depends on ACE2 and TMPRSS2 and Is Blocked by a Clinically Proven Protease Inhibitor. *Cell*. **181**, 271-280.e8
9. Bandres, J. C., Wang, Q. F., O'Leary, J., Baleaux, F., Amara, A., Hoxie, J. A., Zolla-Pazner, S., and Gorny, M. K. (1998) Human Immunodeficiency Virus (HIV) Envelope Binds to CXCR4 Independently of CD4, and Binding Can Be Enhanced by Interaction with Soluble CD4 or by HIV Envelope Deglycosylation. *J. Virol.* **72**, 2500–2504
10. Wu, L., Gerard, N. P., Wyatt, R., Choe, H., Parolin, C., Ruffing, N., Borsetti, A., Cardoso, A. A., Desjardin, E., Newman, W., Gerard, C., and Sodroski, J. (1996) CD4-induced interaction of primary HIV-1 gp120 glycoproteins with the chemokine receptor CCR-5. *Nature*. **384**, 179–183
11. Trkola, A., Dragic, T., Arthos, J., Binley, J. M., Olson, W. C., Allaway, G. P., Cheng- Mayer, C., Robinson, J., Maddon, P. J., and Moore, J. P. (1996) CD4-dependent, antibody-sensitive interactions between HIV-1 and its co- receptor CCR-5. *Nature*. **384**, 184–187
12. Li, Q., Spriggs, M. K., Kovats, S., Turk, S. M., Comeau, M. R., Nepom, B., and Hutt-Fletcher, L. M. (1997) *Epstein-Barr Virus Uses HLA Class II as a Cofactor for Infection of B Lymphocytes*
13. Arenzana-Seisdedos, F., Virelizier, J. L., Rousset, D., Clark-Lewis, I., Loetscher, P., Moser, B., and Baggiolini, M. (1996) HIV blocked by chemokine antagonist. *Nature*. **383**, 400
14. Xia, P., and Dubrovska, A. (2020) Tumor markers as an entry for SARS-CoV-2 infection? *FEBS J.* 10.1111/febs.15499
15. Qi, F., Qian, S., Zhang, S., and Zhang, Z. (2020) Single cell RNA sequencing of 13 human tissues identify cell types and receptors of human coronaviruses. *Biochem. Biophys. Res. Commun.* **526**, 135–140
16. Bar, D. Z., Atkatsh, K., Tavarez, U., Erdos, M. R., Gruenbaum, Y., and Collins, F. S. (2017) Biotinylation by antibody recognition—a method for proximity labeling. *Nat. Methods*. **15**, 127–133
17. Bar, D. Z., Atkatsh, K., Tavarez, U., Erdos, M. R., Gruenbaum, Y., and Collins, F. S. (2018) Addendum: Biotinylation by antibody recognition—a method for proximity labeling. *Nat. Methods*. **15**, 749–749
18. Kim, D. I., and Roux, K. J. (2016) Filling the Void: Proximity-Based Labeling of Proteins in Living Cells. *Trends Cell Biol.* **26**, 804–817
19. Rees, J. S., Li, X.-W., Perrett, S., Lilley, K. S., and Jackson, A. P. (2015) Protein Neighbors and Proximity Proteomics. *Mol. Cell. Proteomics*. **14**, 2848–2856

20. Kotani, N., Gu, J., Isaji, T., Udaka, K., Taniguchi, N., and Honke, K. (2008) Biochemical visualization of cell surface molecular clustering in living cells. *Proc. Natl. Acad. Sci.* **105**, 7405–7409
21. Miyagawa-Yamaguchi, A., Kotani, N., and Honke, K. (2015) Each GPI-anchored protein species forms a specific lipid raft depending on its GPI attachment signal. *Glycoconj. J.* **32**, 531–540
22. Sato, S., Hatano, K., Tsushima, M., and Nakamura, H. (2018) 1-Methyl-4-aryl-urazole (MAUra) labels tyrosine in proximity to ruthenium photocatalysts. *Chem. Commun. (Camb).* **54**, 5871–5874
23. Jiang, S., Kotani, N., Ohnishi, T., Miyagawa-Yamguchi, A., Tsuda, M., Yamashita, R., Ishiura, Y., and Honke, K. (2012) A proteomics approach to the cell-surface interactome using the enzyme-mediated activation of radical sources reaction. *Proteomics*. **12**, 54–62
24. Hashimoto, N., Hamamura, K., Kotani, N., Furukawa, K., Kaneko, K., Honke, K., and Furukawa, K. (2012) Proteomic analysis of ganglioside-associated membrane molecules: Substantial basis for molecular clustering. *Proteomics*. **12**, 3154–3163
25. Ishiura, Y., Kotani, N., Yamashita, R., Yamamoto, H., Kozutsumi, Y., and Honke, K. (2010) Anomalous expression of Thy1 (CD90) in B-cell lymphoma cells and proliferation inhibition by anti-Thy1 antibody treatment. *Biochem. Biophys. Res. Commun.* **396**, 329–334
26. Iwamaru, Y., Kitani, H., Okada, H., Takenouchi, T., Shimizu, Y., Imamura, M., Miyazawa, K., Murayama, Y., Hoover, E. A., and Yokoyama, T. (2016) Proximity of SCG10 and prion protein in membrane rafts. *J. Neurochem.* **136**, 1204–1218
27. Kaneko, K., Ohkawa, Y., Hashimoto, N., Ohmi, Y., Kotani, N., Honke, K., Ogawa, M., Okajima, T., Furukawa, K., and Furukawa, K. (2016) Neogenin, Defined as a GD3-associated Molecule by Enzyme-mediated Activation of Radical Sources, Confers Malignant Properties via Intracytoplasmic Domain in Melanoma Cells. *J. Biol. Chem.* **291**, 16630–16643
28. Kotani, N., Ishiura, Y., Yamashita, R., Ohnishi, T., and Honke, K. (2012) Fibroblast Growth Factor Receptor 3 (FGFR3) Associated with the CD20 Antigen Regulates the Rituximab-induced Proliferation Inhibition in B-cell Lymphoma Cells. *J. Biol. Chem.* **287**, 37109–37118
29. Ohkawa, Y., Momota, H., Kato, A., Hashimoto, N., Tsuda, Y., Kotani, N., Honke, K., Suzumura, A., Furukawa, K., Ohmi, Y., Natsume, A., Wakabayashi, T., and Furukawa, K. (2015) Ganglioside GD3 Enhances Invasiveness of Gliomas by Forming a Complex with Platelet-derived Growth Factor Receptor α and Yes Kinase. *J. Biol. Chem.* **290**, 16043–16058
30. Yamashita, R., Kotani, N., Ishiura, Y., Higashiyama, S., and Honke, K. (2011) Spatiotemporally-regulated interaction between β1 integrin and ErbB4 that is involved in fibronectin-dependent cell migration. *J. Biochem.* **149**, 347–355
31. Kotani, N., Yamaguchi, A., Ohnishi, T., Kuwahara, R., Nakano, T., Nakano, Y., Ida, Y., Murakoshi, T., and Honke, K. (2019) Proximity proteomics identifies cancer cell membrane *cis* -molecular complex as a potential cancer target. *Cancer Sci.* **110**, cas.14108

32. Bojkova, D., Klann, K., Koch, B., Widera, M., Krause, D., Ciesek, S., Cinatl, J., and Münch, C. (2020) Proteomics of SARS-CoV-2-infected host cells reveals therapy targets. *Nature*. **583**, 469–472
33. Chazal, N., and Gerlier, D. (2003) Virus Entry, Assembly, Budding, and Membrane Rafts. *Microbiol. Mol. Biol. Rev.* **67**, 226–237
34. Kotani, N., Nakano, T., Ida, Y., Ito, R., Hashizume, M., Yamaguchi, A., Seo, M., Araki, T., Hojo, Y., Honke, K., and Murakoshi, T. (2018) Analysis of lipid raft molecules in the living brain slices. *Neurochem. Int.* **119**, 140–150
35. Chu, H., Chan, J. F.-W., Yuen, T. T.-T., Shuai, H., Yuan, S., Wang, Y., Hu, B., Yip, C. C.-Y., Tsang, J. O.-L., Huang, X., Chai, Y., Yang, D., Hou, Y., Chik, K. K.-H., Zhang, X., Fung, A. Y.-F., Tsoi, H.-W., Cai, J.-P., Chan, W.-M., Ip, J. D., Chu, A. W.-H., Zhou, J., Lung, D. C., Kok, K.-H., To, K. K.-W., Tsang, O. T.-Y., Chan, K.-H., and Yuen, K.-Y. (2020) Comparative tropism, replication kinetics, and cell damage profiling of SARS-CoV-2 and SARS-CoV with implications for clinical manifestations, transmissibility, and laboratory studies of COVID-19: an observational study. *The Lancet Microbe*. **1**, e14–e23
36. Hamming, I., Timens, W., Bulthuis, M. L. C., Lely, A. T., Navis, G. J., and van Goor, H. (2004) Tissue distribution of ACE2 protein, the functional receptor for SARS coronavirus. A first step in understanding SARS pathogenesis. *J. Pathol.* **203**, 631–637
37. Zhou, P., Yang, X. Lou, Wang, X. G., Hu, B., Zhang, L., Zhang, W., Si, H. R., Zhu, Y., Li, B., Huang, C. L., Chen, H. D., Chen, J., Luo, Y., Guo, H., Jiang, R. Di, Liu, M. Q., Chen, Y., Shen, X. R., Wang, X., Zheng, X. S., Zhao, K., Chen, Q. J., Deng, F., Liu, L. L., Yan, B., Zhan, F. X., Wang, Y. Y., Xiao, G. F., and Shi, Z. L. (2020) A pneumonia outbreak associated with a new coronavirus of probable bat origin. *Nature*. **579**, 270–273
38. Ohnishi, K., Melchers, F., and Shimizu, T. (2005) Lymphocyte-expressed BILL-cadherin/cadherin-17 contributes to the development of B cells at two stages. *Eur. J. Immunol.* **35**, 957–963
39. Bartolomé, R. A., Barderas, R., Torres, S., Fernandez-Aceñero, M. J., Mendes, M., García-Foncillas, J., Lopez-Lucendo, M., and Casal, J. I. (2014) Cadherin-17 interacts with α2β1 integrin to regulate cell proliferation and adhesion in colorectal cancer cells causing liver metastasis. *Oncogene*. **33**, 1658–1669
40. Qiu, H. B., Zhang, L. Y., Ren, C., Zeng, Z. L., Wu, W. J., Luo, H. Y., Zhou, Z. W., and Xu, R. H. (2013) Targeting CDH17 Suppresses Tumor Progression in Gastric Cancer by Downregulating Wnt/β-Catenin Signaling. *PLoS One*. 10.1371/journal.pone.0056959
41. Weigmann, A., Corbeil, D., Hellwig, A., and Huttner, W. B. (1997) Prominin, a novel microvilli-specific polytopic membrane protein of the apical surface of epithelial cells, is targeted to plasmalemmal protrusions of non-epithelial cells. *Proc. Natl. Acad. Sci. U. S. A.* **94**, 12425–12430
42. Filmus, J., and Selleck, S. B. (2001) Glypicans: proteoglycans with a surprise. *J. Clin. Invest.* **108**, 497–501

43. Martin, D. N., and Uprichard, S. L. (2013) Identification of transferrin receptor 1 as a hepatitis C virus entry factor. *Proc. Natl. Acad. Sci. U. S. A.* **110**, 10777–10782

44. Misumi, Y., Hayashi, Y., Arakawa, F., and Ikehara, Y. (1992) Molecular cloning and sequence analysis of human dipeptidyl peptidase IV, a serine proteinase on the cell surface. *BBA - Gene Struct. Expr.* **1131**, 333–336

45. Dreyfuss, G., Matunis, M. J., Pinol-Roma, S., and Burd, C. G. (1993) hnRNP Proteins and the Biogenesis of mRNA. *Annu. Rev. Biochem.* **62**, 289–321

46. Li, Y., Zhang, Z., Yang, L., Lian, X., Xie, Y., Li, S., Xin, S., Cao, P., and Lu, J. (2020) The MERS-CoV Receptor DPP4 as a Candidate Binding Target of the SARS-CoV-2 Spike. *iScience*. **23**, 101160

47. Luo, H., Chen, Q., Chen, J., Chen, K., Shen, X., and Jiang, H. (2005) The nucleocapsid protein of SARS coronavirus has a high binding affinity to the human cellular heterogeneous nuclear ribonucleoprotein A1. *FEBS Lett.* **579**, 2623–2628

48. Spring, F. A., Dalchau, R., Daniels, G. L., Mallinson, G., Judson, P. A., Parsons, S. F., Fabre, J. W., and Anstee, D. J. (1988) The Ina and Inb blood group antigens are located on a glycoprotein of 80,000 MW (the CDw44 glycoprotein) whose expression is influenced by the In(Lu) gene. *Immunology*. **64**, 37–43

49. Shimoda, Y., and Watanabe, K. (2009) Contactins. *Cell Adh. Migr.* **3**, 64–70

50. Takeichi, M. (1991) Cadherin cell adhesion receptors as a morphogenetic regulator. *Science (80-. ).* **251**, 1451–1455

51. Wills, Z. P., Mandel-Brehm, C., Mardinly, A. R., McCord, A. E., Giger, R. J., and Greenberg, M. E. (2012) The nogo receptor family restricts synapse number in the developing hippocampus. *Neuron*. **73**, 466–481

52. Rajan, A., Persson, B. D., Frängsmyr, L., Olofsson, A., Sandblad, L., Heino, J., Takada, Y., Mould, A. P., Schnapp, L. M., Gall, J., and Arnberg, N. (2018) Enteric Species F Human Adenoviruses use Laminin-Binding Integrins as Co-Receptors for Infection of Ht-29 Cells. *Sci. Rep.* 10.1038/s41598-018-28255-7

53. Li, W., Wang, G., Liang, W., Kang, K., Guo, K., and Zhang, Y. (2014) Integrin β3 is required in infection and proliferation of classical swine fever virus. *PLoS One*. 10.1371/journal.pone.0110911

54. Hottz, E. D., Azevedo-Quintanilha, I. G., Palhinha, L., Teixeira, L., Barreto, E. A., Pão, C. R. R., Righy, C., Franco, S., Souza, T. M. L., Kurtz, P., Bozza, F. A., and Bozza, P. T. (2020) Platelet activation and platelet-monocyte aggregates formation trigger tissue factor expression in severe COVID-19 patients. *Blood*. 10.1182/blood.2020007252

55. Tresoldi, I., Sangiuolo, C. F., Manzari, V., and Modesti, A. (2020) SARS-COV-2 and infectivity: Possible increase in infectivity associated to integrin motif expression. *J. Med. Virol.* 10.1002/jmv.25831

56. Kuespert, K., Pils, S., and Hauck, C. R. (2006) CEACAMs: their role in physiology and pathophysiology. *Curr. Opin. Cell Biol.* **18**, 565–571

57. Gray-Owen, S. D., and Blumberg, R. S. (2006) CEACAM1: Contact-dependent control of immunity. *Nat. Rev. Immunol.* **6**, 433–446

58. Krueger, D. K., Kelly, S. M., Lewicki, D. N., Ruffolo, R., and Gallagher, T. M. (2001) Variations in Disparate Regions of the Murine Coronavirus Spike Protein Impact the Initiation of Membrane Fusion. *J. Virol.* **75**, 2792–2802

59. Nunnari, G., Sanfilippo, C., Castrogiovanni, P., Imbesi, R., Li Volti, G., Barbagallo, I., Musumeci, G., and Di Rosa, M. (2020) Network perturbation analysis in human bronchial epithelial cells following SARS-CoV2 infection. *Exp. Cell Res.* 10.1016/j.yexcr.2020.112204

**Table 1. Candidates for protein neighbors of SARS-CoV-2 spike protein in Caco-2 and A549 cell surface**

## Caco-2 cells

| Accession No. | Protein Name | Score* |
|---|---|---|
| Q12864 | Cadherin-17 | 422 |
| P27487 | Dipeptidyl peptidase 4 | 390 |
| O43490 | Prominin-1 (CD133) | 274 |
| Q00839 | Heterogeneous nuclear ribonucleoprotein U | 184 |
| P02786 | Transferrin receptor protein 1 | 160 |
| P11166 | Solute carrier family 2, facilitated glucose transporter member 1 | 68 |
| P35221 | Catenin alpha-1 | 57 |
| P51654 | Glypican-3 | 55 |
| Q9Y3Q0 | N-acetylated-alpha-linked acidic dipeptidase 2 | 51 |
| P12830 | Cadherin-1 | 49 |
| P08195 | 4F2 cell-surface antigen heavy chain | 38 |
| Q9P0L0 | Vesicle-associated membrane protein-associated protein A | 26 |
| P30101 | Protein disulfide-isomerase A3 | 23 |
| P09429 | High mobility group protein B1 | 24 |
| O14672 | Disintegrin and metalloproteinase domain-containing protein 10 | 18 |

## A549 cells

| Accession No. | Protein Name | Score* |
|---|---|---|
| P16070 | CD44 antigen | 153 |
| Q12860 | Contactin-1 | 169 |
| P12830 | Cadherin-1 | 165 |
| Q14002 | Carcinoembryonic antigen-related cell adhesion molecule 7 | 98 |
| Q86UN3 | Reticulon-4 receptor-like 2 | 77 |
| P05556 | Integrin beta-1 | 42 |
| P00533 | Epidermal growth factor receptor | 67 |
| P06731 | Carcinoembryonic antigen-related cell adhesion molecule 5 | 83 |
| P26006 | Integrin alpha-3 | 31 |
| P02786 | Transferrin receptor protein 1 | 64 |

* From the search engine (Proteome Discoverer 2.4 software).

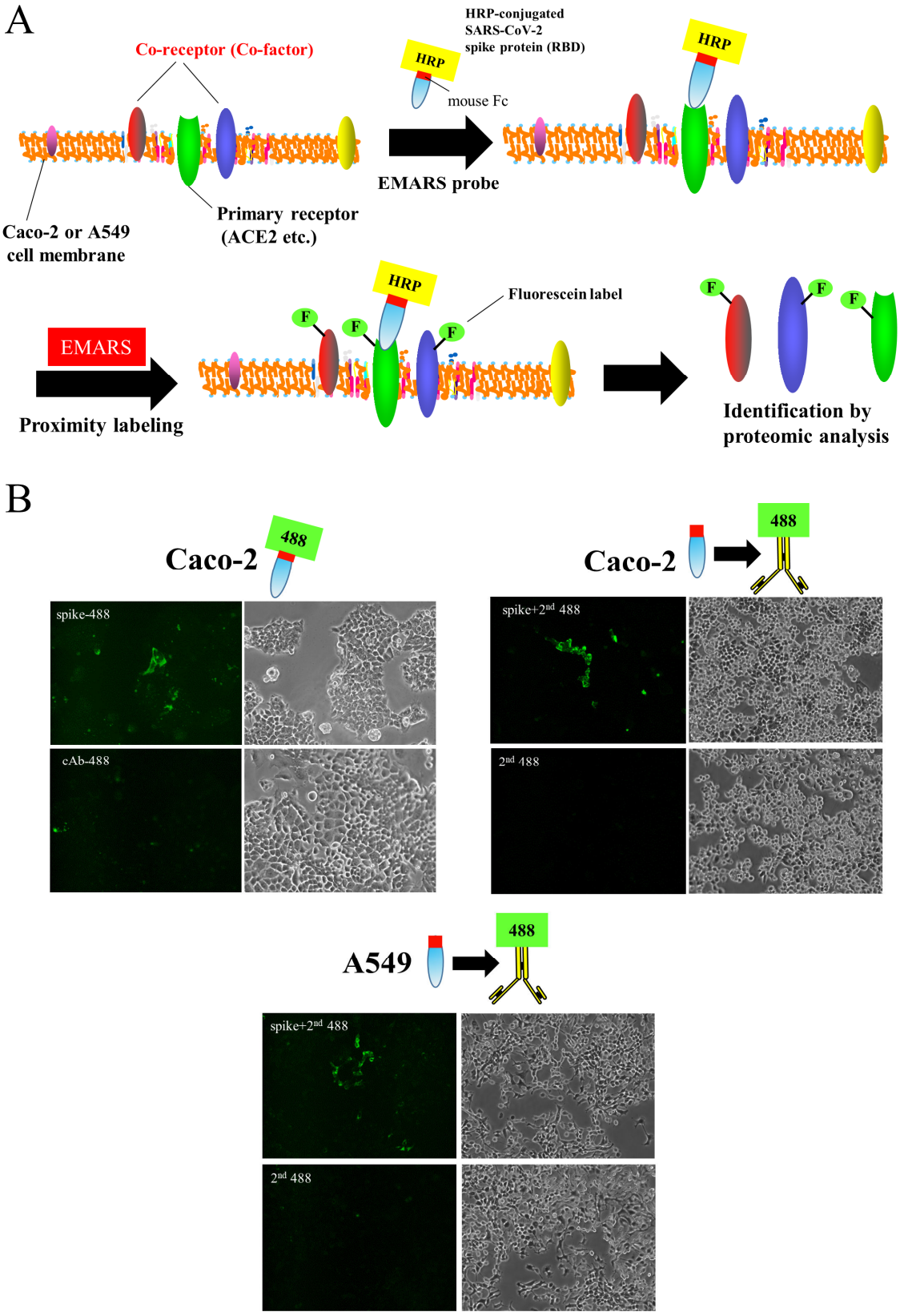


**Fig. 1 Schematic of the screening for candidate membrane proteins involved in SARS-CoV-2 entry**
(*A*) Schematic illustration of the labeling procedure according to EMARS. Prior to the EMARS reaction, Fluorescein-labeled proteins were purified and then analyzed using mass spectrometry. (*B*) Immunocytochemical staining of SARS-CoV-2 spike proteins in Caco-2 and A549 cells. The staining of monovalent Alexa Fluor 488-labeled spike proteins (Spike-488) and the two step staining (spike protein followed by Alexa Fluor 488 secondary antibody; spike+2$^{nd}$ 488) were performed with DIC images. Negative control samples (cAB-488 or 2$^{nd}$ 488) were also prepared simultaneously.

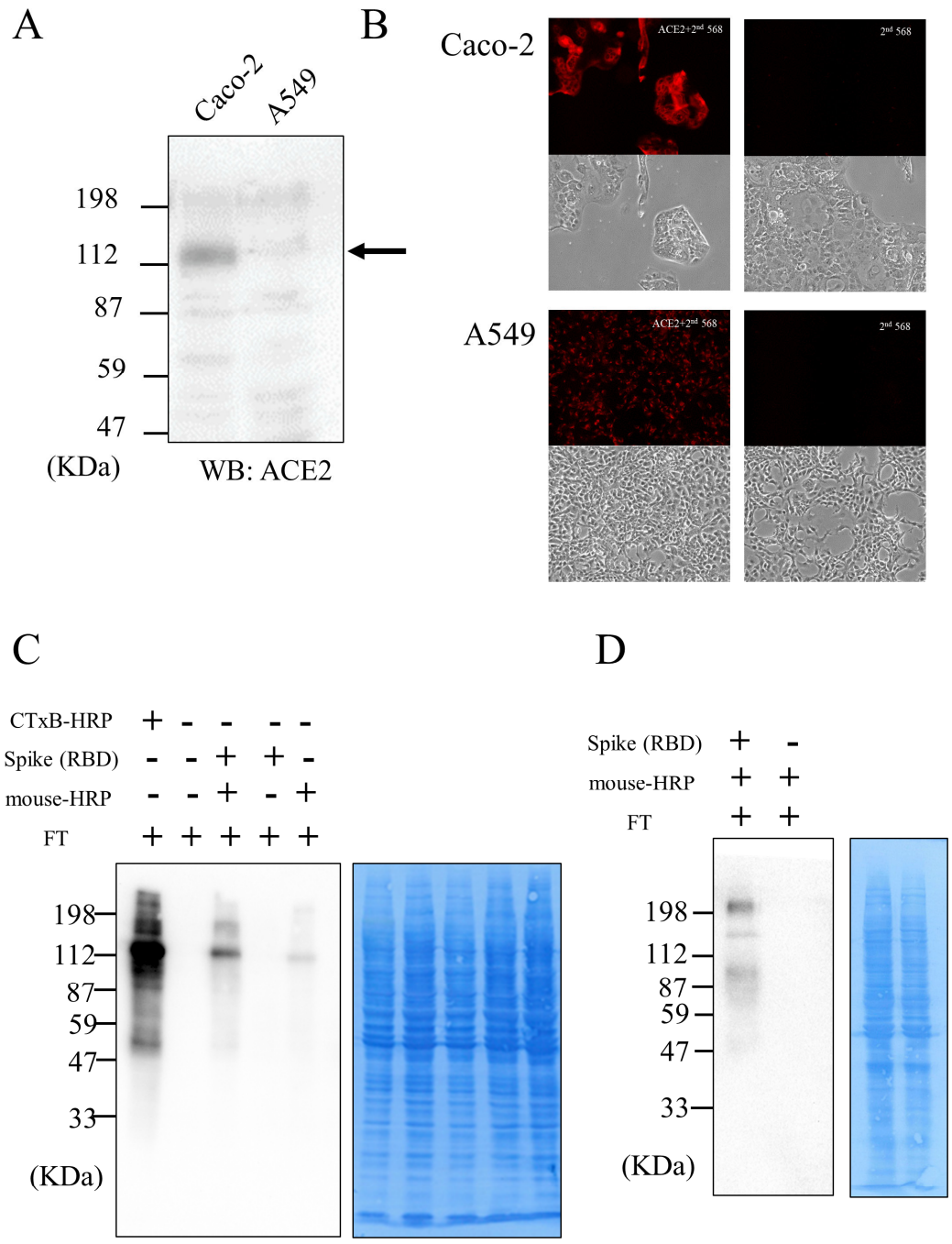


**Fig. 2 Proximity labeling near cell membrane-bound SARS-CoV-2 spike protein**
(*A*) ACE2 expression in Caco-2 and A549 cells. Western blot analysis of Caco-2 and A549 cell lysates (10µg protein each) were subjected to SDS-PAGE (10 % gel) and stained with anti-ACE2 antibody. Arrows indicate the bands of the ACE2 protein. (*B*) Immunocytochemical staining of ACE2 protein in Caco-2 and A549 cells. The staining with anti-ACE2 antibody (ACE2+2$^{nd}$ 568) was performed with DIC images. Negative control samples (2$^{nd}$ 568) were also prepared simultaneously. (*C, D*) Protein neighbors of cell membrane-bound SARS-CoV-2 spike proteins. The EMARS reaction described in the "Experimental procedure" was performed in Caco-2 (*C*) and A549 (*D*) cells using a spike protein (*Spike (RBD)*) and HRP-conjugated anti-mouse IgG (*mouse HRP*). The EMARS products were subsequently subjected to Western blot analysis to detect fluorescein-labeled proteins as protein neighbors. In Caco-2 cells, HRP-conjugated Cholera Toxin B Subunit B (*CTxB-HRP*) was also used for the EMARS reaction as a positive control. For loading controls, the PVDF membrane was stained with Coomassie Brilliant Blue solution (right column)

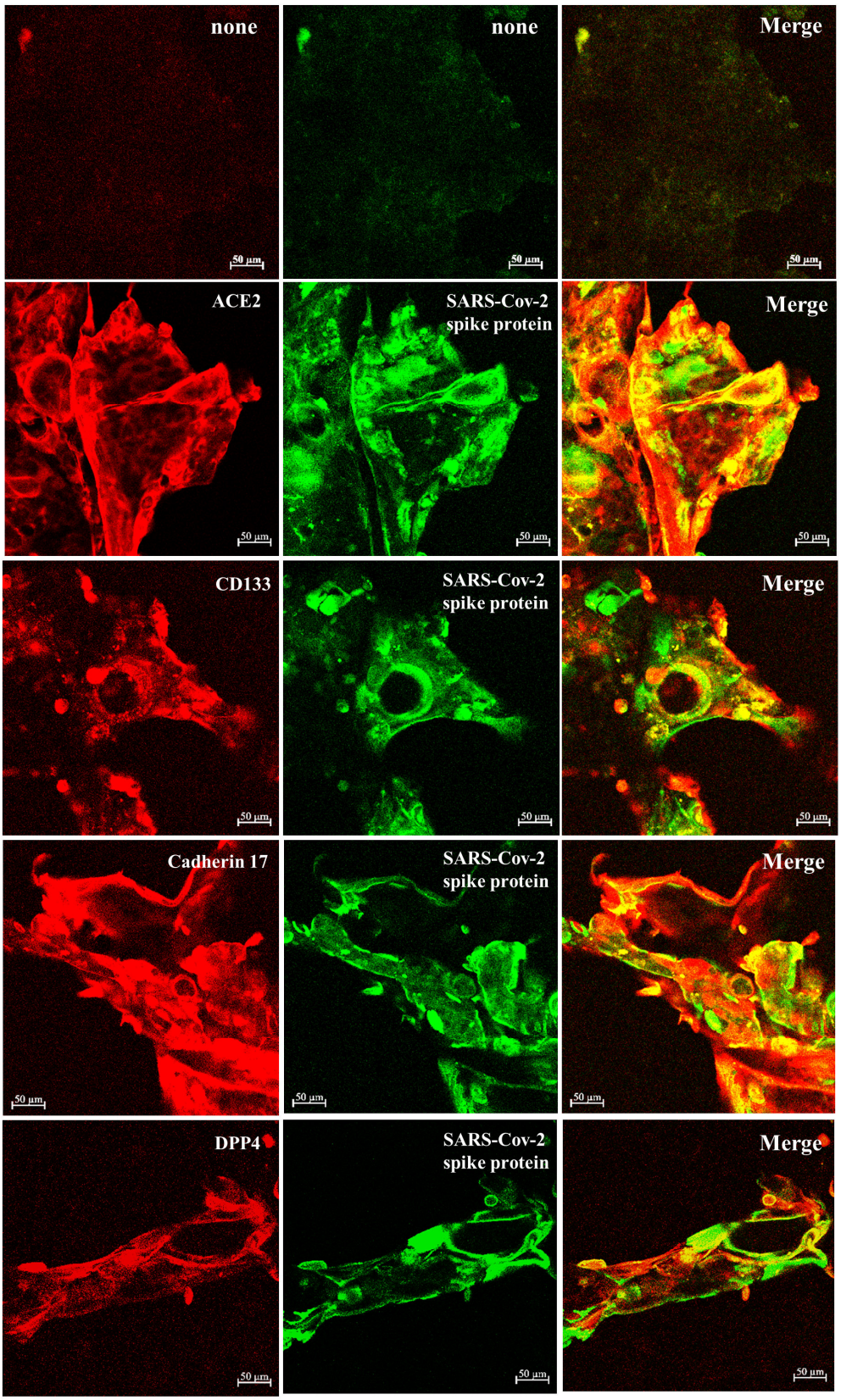


**Fig. 3 Co-localization of identified proteins with cell membrane-bound SARS-CoV-2 spike proteins**
Representative images of co-localization with SARS-CoV-2 spike proteins and the identified membrane proteins. Caco-2 cells were co-stained for SARS-CoV-2 spike protein (green; middle column) and the antibodies recognizing ACE2, CD133, Cadherin 17, and DPP4, respectively (Red; left column). Then, the resulting specimens were stained with appropriate secondary antibodies and subsequently observed using confocal microscopy (x20 objective). Co-localization was indicated as yellow in the "Merge" images (right column).